UCSF
UC San Francisco Previously Published Works

Title

GABAB receptors in maintenance of neocortical circuit function

Permalink

https://escholarship.org/uc/item/6zt9g14t

Authors

Sebe, Joy Y

Looke-Stewart, Elizabeth

Baraban, Scott C

Publication Date

2014-11-01

DOI

10.1016/j.expneurol.2014.05.018

Peer reviewed

Regular Article

GABA_B receptors in maintenance of neocortical circuit function

Joy Y. Sebe [a], Elizabeth Looke-Stewart [a], Scott C. Baraban [a,b,c,*]

[a] Department of Neurological Surgery, University of California, San Francisco, San Francisco, CA 94143, USA
[b] Graduate Program in Neuroscience, University of California, San Francisco, San Francisco, CA 941432, USA
[c] The Eli and Edythe Broad Center of Regeneration Medicine and Stem Cell Research, University of California, San Francisco, San Francisco, CA 94143, USA

ABSTRACT

Activation of metabotropic GABA$_B$ receptors (GABA$_B$Rs) enhances tonic GABA current and substantially increases the frequency of spontaneous seizures. Despite the and pro-epileptic consequences of GABA$_B$R activation, mice lacking functional GABA$_B$ receptors (GABA$_{B1}$R KO mice) exhibit clonic and rare absence seizures. To examine these mutant mice further, we recorded excitatory and inhibitory synaptic inputs and tonic mutant GABA currents from Layer 2 neocortical pyramidal neurons of GABA$_{B1}$R WT and KO mice (P30–40). Tonic current was increased while the frequency of synaptic inputs was unchanged in KO mice relative to WT littermates. The neocortical laminar distribution of interneuron subtypes derived from the medial ganglionic eminence (MGE) was also not statistically different in KO mice relative to WT while the number of calretinin-positive, caudal GE-derived cells in Layer 1 was reduced. Transplantation of MGE progenitors obtained from KO mice lacking functional GABA$_{B1}$R did not increase tonic inhibition in the host brain above that of media-injected controls. Taken together, these results suggest a complex role for GABA$_B$ receptors in mediating neocortical circuit function.

© 2014 Elsevier Inc. All rights reserved.

Introduction

Disruptions in GABA-mediated inhibition following defects in interneuron development (Marsh et al., 2009; Powell et al., 2003; Wang et al., 2010), firing (Cheah et al., 2012) or survival (Cobos et al., 2005) lead to increased cortical excitability and spontaneous electrographic seizures. That a reduction in GABA-mediated inhibition is pro-epileptic is further supported by work demonstrating that electrographic seizures are suppressed by enhancing inhibition or interneuron activity via pharmacological (Macdonald and Kelly, 1995), optogenetic (Krook-Magnuson et al., 2013) or cell transplantation (Baraban et al., 2009; Hunt et al., 2013) approaches.

The effects of GABA-mediated inhibition on neural circuit function are multifaceted. While many antiepileptic medications act by increasing synaptic GABAergic current (Meldrum and Rogawski, 2007), elevated levels of extrasynaptic GABA current are associated with epilepsy (Cope et al., 2009). Increased levels of tonic GABA inhibition, mediated by high-affinity extrasynaptic GABA$_A$ receptors (GABA$_A$Rs) (Farrant and Nusser, 2005), are observed in genetic rodent models of absence epilepsy (Cope et al., 2009) and administration of an extrasynaptic GABA$_A$R agonist leads to electrographic absence seizures in normal rats (Fariello and Golden, 1987).

Aside from the ionotropic GABA$_A$Rs, metabotropic GABA$_B$ receptors (GABA$_B$Rs), which have long been known to decrease the release of

excitatory and inhibitory neurotransmitters, and to hyperpolarize neurons by activating a K$^+$ efflux (Dutar and Nicoll, 1988; Newberry and Nicoll, 1984; Thompson and Gähwiler, 1989), also affect the severity of absence seizures. GABA$_B$R activation directly increases tonic current amplitude via an intracellular modulation of extrasynaptic GABA$_A$Rs (Connelly et al., 2013). Administration of GABA$_B$R agonists exacerbates absence seizures and that of antagonists suppresses absence seizures (Hosford et al., 1992). Based on these data, one would expect mice lacking functional GABA$_B$Rs to be resistant to absence seizures. However, GABA$_{B1}$R knockout (KO) mice, which lack the B1 receptor subunit that is required to bind GABA, do not express functional GABA$_B$Rs and exhibit rare but spontaneous absence and tonic–clonic electrographic seizures (Schuler et al., 2001). In contrast to WT mice, hippocampal pyramidal cells from GABA$_{B1}$R KO mice do not exhibit presynaptic inhibition of GABA or glutamate release, or an outward current, in response to the GABA$_B$R agonist baclofen (Schuler et al., 2001). In behavioral assays these mice exhibit hyperlocomotor and hyperalgesic activity suggesting that GABA$_B$Rs play a critical role in the circuit function underlying locomotion and nociception. These mutants offer an opportunity to explore the function of GABA$_B$ receptors in the neocortex.

Here we used a combination of electrophysiological and immunohistochemical approaches to determine whether the lack of functional GABA$_B$Rs alters synaptic or extrasynaptic transmission as well as interneuron differentiation and distribution in the neocortex. An MGE cell transplantation assay (Alvarez-Dolado et al., 2006) was used to determine whether elevated levels of tonic inhibition observed in GABA$_{B1}$R KO mice translated to increased levels of tonic inhibition in WT graft recipients that had received interneuron progenitors derived from

embryonic KO mice. Lastly, to further examine the relationship between MGE-derived interneurons, $GABA_BRs$ and tonic inhibition in the host brain, we grafted increasing numbers of WT progenitors into the neocortex and measured tonic currents from pyramidal cells of graft recipients.

Materials and methods

Animals

All animal procedures were performed in accordance with the UCSF Institutional Animal Care and Use Committee guidelines. BALB/cJ $GABA_{B1}R^{+/-}$ mice (Schuler et al., 2001) (gift from Bernhard Bettler, University of Basel) were mated with actin-GFP$^+$ mice to generate $GABA_{B1}R^{+/+}$:GFP and $GABA_{B1}R^{-/-}$:GFP, which we refer to as WT and $GABA_{B1}R$ KO, respectively. For all transplantation studies, GFP$^+$ cells were grafted into WT CD-1 mice (Charles River, Harlan). Cells were transplanted into CD-1 mice given that the anatomical and functional integration of grafted progenitor cells is well-established in CD-1 host mice (Alvarez-Dolado et al., 2006; Baraban et al., 2009; Sebe et al., 2013).

Immunohistochemistry and cell counts

Brains of $GABA_{B1}R$ KO mice ($GABA_{B1}R^{-/-}$:GFP) and WT ($GABA_{B1}R^{+/+}$:GFP) littermates were fixed in 4% paraformaldehyde by perfusion and 50 μm coronal sections were cut by vibratome. Floated sections were labeled for parvalbumin (PV: Sigma P3088; 1:500), somatostatin (SOM: Santa Cruz 7819; 1:500), neuropeptide Y (NPY: ImmunoStar 22940; 1:500) or calretinin (CR: Millipore AB5054; 1:500). Following the application of one of these primary antibodies, diaminobenzidine (DAB; Sigma) staining was performed using the ABC elite kit (Vector Labs). Slices were mounted and dehydrated with a series of washes in ethanol and xylenes. Counts of interneuron subtypes were conducted by an investigator blind to genotype. To conduct cell counts, bright field images of slices containing somatosensory cortex were captured and images of slices were reconstructed in Adobe Illustrator (Adobe Systems Inc.). For each pair of WT and KO littermates, slices containing the same regions of somatosensory cortex were marked by rectangles of the same dimensions and area. DAB-positive cells contained in these rectangles were counted in each neocortical layer. For each mouse, at least two brain slices were used to conduct cell counts. Data are reported in two ways: (1) mean percent of an interneuron subtype in each neocortical layer relative to the total number of cells counted for each mouse (Figs. 3e–h) and (2) density of an interneuron subtype within a given area of somatosensory cortex that spanned all neocortical layers (Fig. 3i).

Electrophysiology

Coronal brain slices (300 μm) were prepared in a high sucrose solution, incubated (35 °C for 30 min) and perfused with 33–34 °C ACSF containing (in mM): 124 NaCl, 3 KCl, 1.25 NaH2PO4–H2O, 2 MgSO4–7H2O, 26 NaHCO3, 10 dextrose, and 2 CaCl2. For all recordings of synaptic and tonic currents, patch electrodes (3 MΩ) were filled with (in mM): 140 CsCl, 1 MgCl2, 10 HEPES, 11 EGTA, 2 NaATP, and 0.5 Na2GTP. To record spontaneous excitatory or inhibitory postsynaptic currents from $GABA_{B1}R$ WT or KO cells, slices were perfused with the $GABA_AR$ antagonist gabazine (100 μM) (Sigma) or glutamate receptor antagonists APV (25 μM) and DNQX (20 μM) (Sigma). TTX (1 μM, Alomone Labs) was also added to the bath perfusate to record miniature synaptic currents. To record tonic GABA currents, slices were treated with the APV (25 μM) and DNQX (20 μM) (Sigma). To block GABA uptake, slices were perfused with the GABA transporter 1 (GAT1) and GABA transporter 2/3 (GAT2/3 antagonists) NO-711 (20 μM, Sigma) and SNAP5114 (100 μM, Tocris). When the holding current stabilized (4–5 min), gabazine (100 μM) was applied to the bath. Tonic current

was measured by finding the mean holding current of trace sections that were free of synaptic events before and after $GABA_AR$ blockade (Sebe et al., 2010). The standard deviation of the holding current, which is equivalent to the RMS noise (square root of the variance), was used to measure current noise. Measuring changes in current noise before and after $GABA_AR$ blockade is a way to assess changes in the activity of open $GABA_ARs$ (Bright and Smart, 2013). The percent change in the standard deviation (SD) of the holding current was calculated by measuring the standard deviation in a section free of synaptic activity before and after $GABA_AR$ blockade. To obtain the data in Fig. 6, in which we recorded tonic current from slices that had received increasing doses of GFP+ grafted cells, we filled the recorded host pyramidal cell with Alexa Fluor 594. After each recording, the red fluorescing cell in the live slice was placed in the center of the 40× field of view (area of field of view = 0.23 mm^2) and the number of GFP$^+$ cells in this field counted. To characterize firing patterns and record sEPSCs from grafted derived GFP$^+$ cells, patch electrodes were filled with (in mM): 140 KGluconate, 1 NaCl, 5 EGTA, 10 HEPES, 1 MgCl2, 1 CaCl2, 2 Na-ATP and Alexa Fluor 594 to fill the recorded cell. Excitatory synaptic currents were recorded in the presence of gabazine. Series resistance was measured after each recording and data were discarded if the resistance changed by more than 20% or if the series resistance was >20 MΩ. For all voltage-clamp recordings, data were acquired using Clampex software (Molecular Devices, Sunnyvale, CA) at a gain of 5, sampling rate of 5 kHz and holding potential of −60 mV. For current-clamp recordings, data were acquired at a gain of 5 and a 10 kHz sampling rate. Current steps (1 s) of varying amplitudes were injected into the cell to determine the threshold for firing and the cell's firing frequency. Firing frequency was defined as the firing frequency at double the current necessary to depolarize the cell to threshold. MiniAnalysis Software (Synaptosoft, Inc.) was used to measure the frequency, amplitude and decay of synaptic currents. Unpaired t-tests were used to compare the characteristics of synaptic and tonic currents between WT and KO cells. Two way ANOVAs (Tukey posthoc test) were used to compare the characteristics of tonic currents recorded from host cells in mice that had received media injection (control), WT grafted or KO grafted cells. Statistical significance for all tests was defined as a p < 0.05.

Transplantation

For transplantation studies, interneuron progenitors were isolated from a well-studied embryonic structure termed the medial ganglionic eminence (MGE) (Marin and Rubenstein, 2001; Wichterle et al., 1999). The anterior portion of MGE was dissected from E12.5 GFP-expressing mouse embryos and placed in a mixture of L-15 media (UCSF Cell Culture Facility) and DNAse (Qiagen, Valencia, CA). In all studies, GFP$^+$ MGE cells were unilaterally injected into neocortices of postnatal day 3 (P3) WT CD-1 mice. A single "MGE" refers to MGE tissue obtained from one hemisphere of the embryonic brain and is thereby half of the total MGE cells in a donor embryo. For studies comparing host brain tonic current following the transplantation of WT vs. KO MGE cells, 2 MGEs were front-loaded into an injection needle containing media (outer diameter 70–80 μm) and injected 700 μm deep into the somatosensory cortex to target Layer 6. Cells were injected into 2 different sites. For studies in which we examined tonic current following the transplantation of increasing numbers of MGE cells, we injected 1–4 MGEs in 3 different sites, again into Layer 6. In all studies, graft recipients were sacrificed 30–40 days after transplantation (DAT).

Assessing MGE cell viability

To count the number of living and dead cells in a single dissected MGE, we used two methods. First, we counted the total number of dissected cells prior to loading cells into the injection needle. MGE was dissociated in media containing DNAse, combined with equal parts of

trypan blue, and loaded into a hemocytometer. Using this method, there were 180,000 to 200,000 cells in each MGE and 80–90% of these cells were alive i.e., trypan blue negative (144,000–180,000 cells). Second, we counted the number of cells after a single MGE had been loaded into the injection needle and all visible cells were ejected into a 100 μL drop of media. The total cell count and viability decreased after needle loading. After needle loading, we counted 138,000–142,000 cells in each MGE and 50–70% of these cells were alive. Therefore, for each MGE loaded into the needle, we estimate an injection of approximately 69,000–99,000 live cells.

Results

Excitatory and inhibitory synaptic transmission, and tonic GABA current in GABA$_{B1}$ receptor KO mice

Using young adult GABA$_{B1}$R$^{-/-}$ mice, we first confirmed that KO mice lack functional GABA$_B$Rs. In voltage-clamp mode, we recorded spontaneous inhibitory postsynaptic currents (sIPSCs) from L2 neocortical pyramidal cells in acute slices prepared from KO or age-matched WT sibling controls. IPSCs were monitored at baseline and after bath application of baclofen (50 μM), a GABA$_B$R agonist (Scanziani et al., 1992). As expected (Schuler et al., 2001), baclofen significantly reduced sIPSC frequency on WT cells (baseline: 15 ± 2 Hz; baclofen: 8 ± 1 Hz; n = 5 cells per genotype; p < 0.01, paired t-test) but had no effect on sIPSCs recorded from KO cells (baseline: 13 ± 2 Hz; baclofen: 13 ± 2 Hz; n = 5 cells per genotype). Next we recorded excitatory and inhibitory postsynaptic currents (EPSCs and IPSCs) in acute neocortical slices from both mouse genotypes (P30–45) (Table 1). Miniature EPSC (mEPSC) mean frequency and decay times were not different while amplitude was reduced to ~25% in KO mice (Fig. 1). As shown in Figs. 2b–d and Table 1, miniature IPSC (mIPSC) mean frequency, amplitude and decay time were not significantly different. Because tonic current recordings described below were conducted in the presence of action potential dependent inhibitory synaptic activity, we also compared sIPSCs in slices from WT and KO mice (Figs. 2f–h). Spontaneous IPSC (sIPSC) frequency and amplitude were not different, but decay time was reduced to ~25% in KO mice. Next, we analyzed mean tonic current in the presence of GAT1 and 2/3 blockers followed by bath application of the GABA$_A$R antagonist gabazine. Bath perfusion of both of these GABA transporter blockers is necessary to reveal tonic currents recorded from neocortical neurons in the acute brain slice (Keros and Hablitz, 2005). Interestingly, mean tonic current was significantly increased in pyramidal cells from KO animals (WT: 102 ± 17 pA, n = 15; KO: 162 ± 23 pA, n = 15; unpaired t-test, p < 0.05) (Figs. 2i–k) while the percent change in the standard deviation was unchanged (WT: −60 ± 4%, n = 15; KO: −62 ± 4%, n = 15; n.s.) (Fig. 2l).

To address whether the tonic inhibition increase could be due to a difference in interneuron numbers or distribution, we examined the density and neocortical laminar distribution of PV$^+$, SOM$^+$ and NPY$^+$ cells in WT and KO mice at P30–45. In both genotypes, the density of PV$^+$ (WT: 0.19 ± 0.02 cells/mm^2; KO: 0.21 ± 0.01 cells/mm^2; n.s., n = 5 for each genotype), SOM$^+$ (WT: 0.18 ± 0.01 cells/mm^2; KO: 0.17 ± 0.03 cells/mm^2; n.s., n = 5 for each genotype) and NPY$^+$ cells (WT: 0.06 ± 0.02 cells/mm^2; KO: 0.06 ± 0.02 cells/mm^2; n.s., n = 5 for
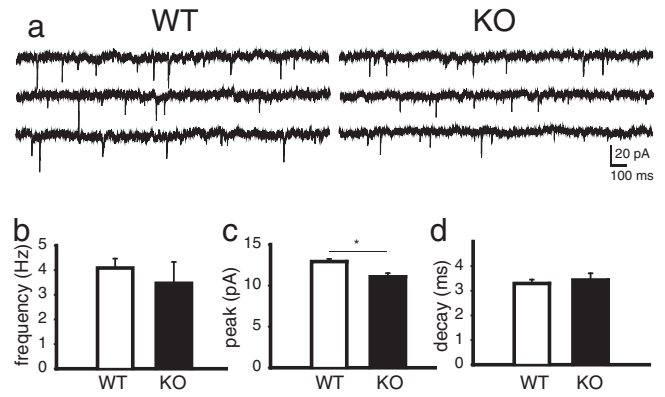
Fig. 1. Miniature EPSCs recorded from GABA$_{B1}$R WT and KO mice. a) Representative raw traces of mEPSCs from GABA$_{B1}$R WT (left) and KO (right) mice. b–d. Summary histograms show that mEPSC mean frequency and decay are not significantly different between WT and KO mice, whereas mean peak amplitude recorded from KO mice is significantly lower than WT (*, p < 0.01; un-paired t-test, n = 16 per genotype).

each genotype) was not statistically different (Fig. 3i). As expected (Ciceri et al., 2013; Miyoshi and Fishell, 2011; Sebe et al., 2013), PV$^+$ and SOM$^+$ interneuron subtypes in WT mice localized to deeper neocortical layers with few to no cells in L1 (Figs. 3a, b, e, f); NPY$^+$ cells were most prominent in L2/3, 5 and 6 (Figs. 3c, g). The density and distribution of these interneuron sub-populations were not regulated by GABA$_B$Rs as similar patterns were noted in both WT and receptor KO mice. CR$^+$ cells, which primarily originate in CGE (Miyoshi et al., 2007, 2010; Nery et al., 2002), were located in more superficial layers (Figs. 3d, h), as expected. Interestingly, the percentage of CR$^+$ cells in L1 was reduced in the KO neocortex (WT: 16 ± 2%; KO: 7 ± 2%; n = 4; p < 0.05, Two-way ANOVA, Tukey posthoc). In both genotypes, the density of CR$^+$ cells (WT: 0.029 ± 0.006 cells/mm^2; KO: 0.021 ± 0.004 cells/mm^2; n.s., n = 4 for each genotype) was not statistically different (Fig. 3i).

Grafted GABA$_{B1}$R KO function in the recipient neocortex

MGE progenitor cell transplantation into the WT neocortex increases tonic GABA currents recorded from host brain neocortical pyramidal cells (Baraban et al., 2009). Given that tonic currents in the GABA$_{B1}$R KO neocortex are elevated relative to WT, we tested whether grafting interneuron progenitors from KO donors increases host brain tonic currents beyond levels observed following the normal transplantation of WT MGE cells. Because GABA$_B$Rs have been implicated in interneuron development (Behar et al., 2001), we first assessed whether graft-derived interneurons from KO donors can mature into electrically active neurons. GFP fluorescence was used to identify graft-derived interneurons in acute neocortical tissue slices at 30–40 days after transplantation (DAT) (Fig. 4a). In current-clamp mode, the majority of GFP$^+$ patched cells were fast-spiking interneurons that fired at a frequency of >100 Hz when injected with twice the minimal current necessary to elicit an action potential (Figs. 4b, c), consistent with previously reported firing properties of MGE-derived interneurons (Alvarez-Dolado et al., 2006; Baraban et al., 2009; Hunt et al., 2013). In addition, EPSCs could be recorded in all GFP$^+$ cells (n = 7; Figs. 4d, e) suggesting that graft-derived cells are synaptically integrated (Martinez-Cerdeno et al., 2010).

Next, we measured tonic current in acute neocortical slices from mice injected with media only, WT or KO MGE progenitor cells (Fig. 5). Tonic currents were recorded in the presence of GABA transporter blockers, NO711 and SNAP5114. In pyramidal neurons from mice receiving WT MGE progenitor cell grafts (30–40 DAT), tonic current was increased as expected (n = 10; Figs. 5b, d). Surprisingly, a similar increase in tonic current was not observed in mice receiving KO

Table 1
Postsynaptic currents from GABAB1R WT vs. KO L2 pyramidal cells.

		Frequency (Hz)	Amplitude (pA)	Decay (ms)	N
mEPSC	WT	4 ± 0.4	12.9 ± 0.3[a]	3.3 ± 0.2	16
	KO	3.5 ± 0.9	11.1 ± 0.4[a]	3.4 ± 0.3	16
mIPSC	WT	10 ± 1	37 ± 2	6 ± 0.7	15
	KO	10 ± 2	39 ± 2	6 ± 0.3	15
sIPSC	WT	17 ± 2	33 ± 5	4.2 ± 0.4	15
	KO	20 ± 2	38 ± 3	3.2 ± 0.2	16

[a] Indicates that the values were significantly different, p < 0.01; un-paired t-test.
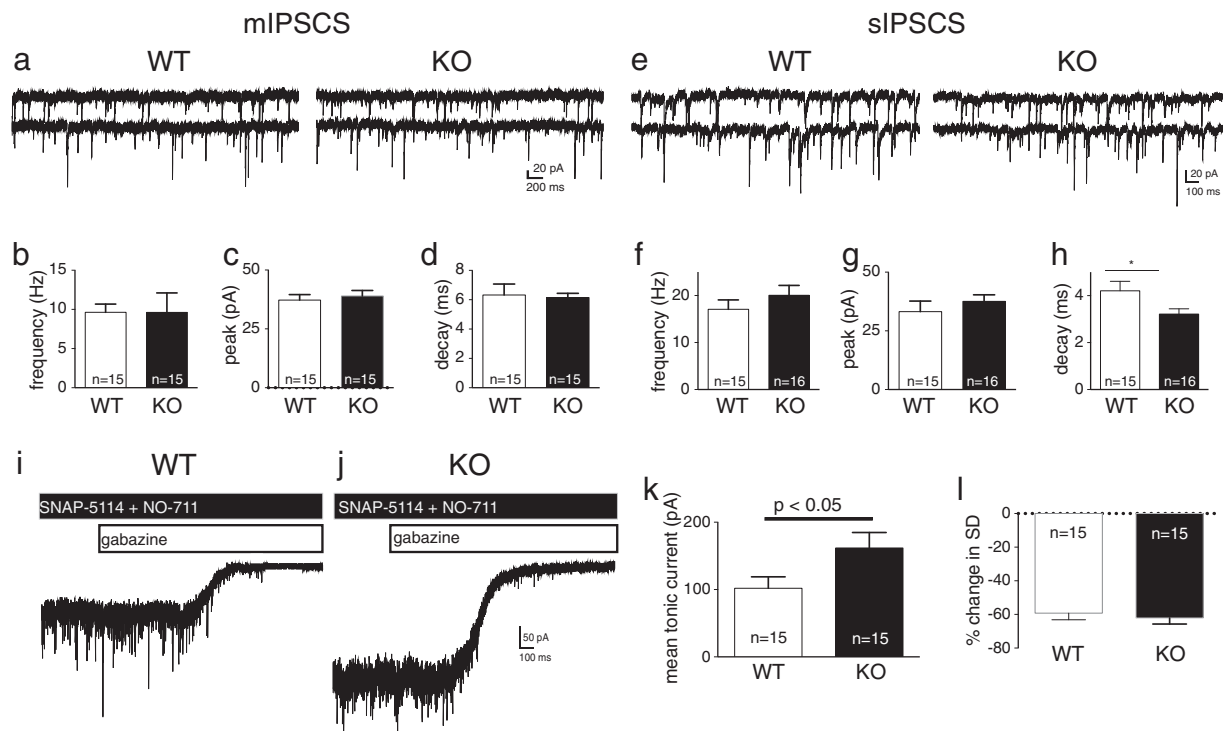
Fig. 2. Extrasynaptic, not synaptic inhibition, is elevated in neocortical neurons of GABA$_{B1}$R KO mice. a) Representative raw traces of mIPSCs from GABA$_{B1}$R WT (left) and KO (right) mice. b–d. Summary histograms show that mIPSC mean frequency and decay are not significantly different between WT and KO mice. e) Representative raw traces of sIPSCs from GABA$_{B1}$R WT (left) and KO (right) mice. f–g. Summary histograms show that sIPSC mean frequency and peak are not significantly different between WT and KO mice whereas mean decay time recorded from KO mice is significantly lower than WT (*, p < 0.01; un-paired t-test). i, j) Representative raw traces of tonic currents reflect the increase in mean tonic current in KO mice (k; *, p < 0.01; un-paired t-test). The percent change in the standard deviation following bath application of gabazine was not statistically different between WT and KO mice.

MGE cell grafts (n = 8; Figs. 5c, d). The standard deviation of the holding current was unchanged in these experiments (Fig. 5e).

We have previously shown that transplanting WT MGE cells into the WT mouse neocortex increases the frequency of inhibitory synaptic events recorded from host brain pyramidal cells. However, increasing the dosage of transplanted MGE cells, and thereby the density of grafted cells in the host brain, does not further increase synaptic inhibition (Southwell et al., 2012). To determine whether tonic inhibition scales upward with the number of MGE-derived cells in the recipient neocortex, we recorded tonic currents in mice that received increased doses of MGE cells. In acute neocortical slices from WT graft recipients (30–40 DAT), we analyzed tonic current on L2/3 pyramidal cells in voltage-clamp recordings. To measure "maximal" tonic currents in the presence of endogenously released GABA, we blocked GAT1 and 2/3 via bath application of NO711 and SNAP5114, respectively, and added the GABA$_A$R blocker gabazine (Figs. 6a, b). At the end of each recording, we counted the number of neighboring GFP$^+$ cells in the field of view. Fig. 6b shows a representative recording from a L2 pyramidal cell with only one GFP$^+$ cell in the field of view (see schematic to the left of Fig. 6a). When the recorded pyramidal cell is surrounded by more GFP$^+$ cells, tonic currents are significantly increased (Fig. 6b). A scatter plot shows that tonic currents increase linearly as a function of the number of neighboring MGE-derived GFP$^+$ cells (Fig. 6c; p = 0.002, Spearman Rank Correlation Coefficient = 0.51). The standard deviation of the holding current reflects current fluctuations due to the opening and closing of GABA$_A$Rs (Sebe et al., 2010). The percent change in the SD of the holding current also increased as a function of the number of neighboring GFP$^+$ cells (Fig. 6d; p = 0.006; Spearman Rank Correlation Coefficient = 0.46). However, when these experiments were performed under more physiological conditions (e.g., in the absence of re-uptake blockers and gabazine), there was no detectable tonic current regardless of the number of neighboring GFP$^+$ cells. Representative traces recorded from L2/3 host pyramidal cells in the same field of

view as 1 and 14 GFP$^+$ cells are shown (Figs. 6a′ and b′, respectively). As the number of neighboring GFP$^+$ cells increases, tonic currents remain below levels of detection. Although not shown in Fig. 6, even a host pyramidal neuron with 19 GFP$^+$ cells within the field of view had an insignificant tonic current of −1 pA and no change in the SD of the holding current.

Discussion

Principal findings of our experiments are as follows. GABA$_{B1}$R KO mice do not exhibit changes in the frequency of excitatory or inhibitory synaptic transmission. GABA$_{B1}$R KO mice exhibit an increase in tonic current not accompanied by changes in the number or neocortical laminar distribution of PV$^+$, SOM$^+$ and NPY$^+$ interneurons. A significant reduction in the number of CR$^+$, CGE-derived, cells in KO mice in the superficial layers of the neocortex was noted. No increase in tonic current was observed when MGE progenitor cells from these KO animals were grafted into the WT neocortex. Mean tonic current recorded in the presence of GABA uptake blockers scales upward with the number of neighboring grafted cells.

Enhancement of tonic current in the absence of GABA$_B$Rs

Our electrophysiological data from acute neocortical tissue slices suggest that the mean amplitude of tonic current (but not the amplitude, frequency or decay of inhibitory synaptic currents) is elevated in GABA$_{B1}$R KO mice. This increase in tonic current may be due to an increase in the effectiveness and/or number of GABA transporters. If more "efficient" GABA transporters are blocked in slices from KO mice, then the amount of extrasynaptic GABA would increase relative to WT slices leading to an elevation in mean tonic current, as observed. Alternatively, an increase in tonic current may be linked to the reduction in CR$^+$ interneurons in L1 of these animals. CR$^+$ terminals in L2/3, the
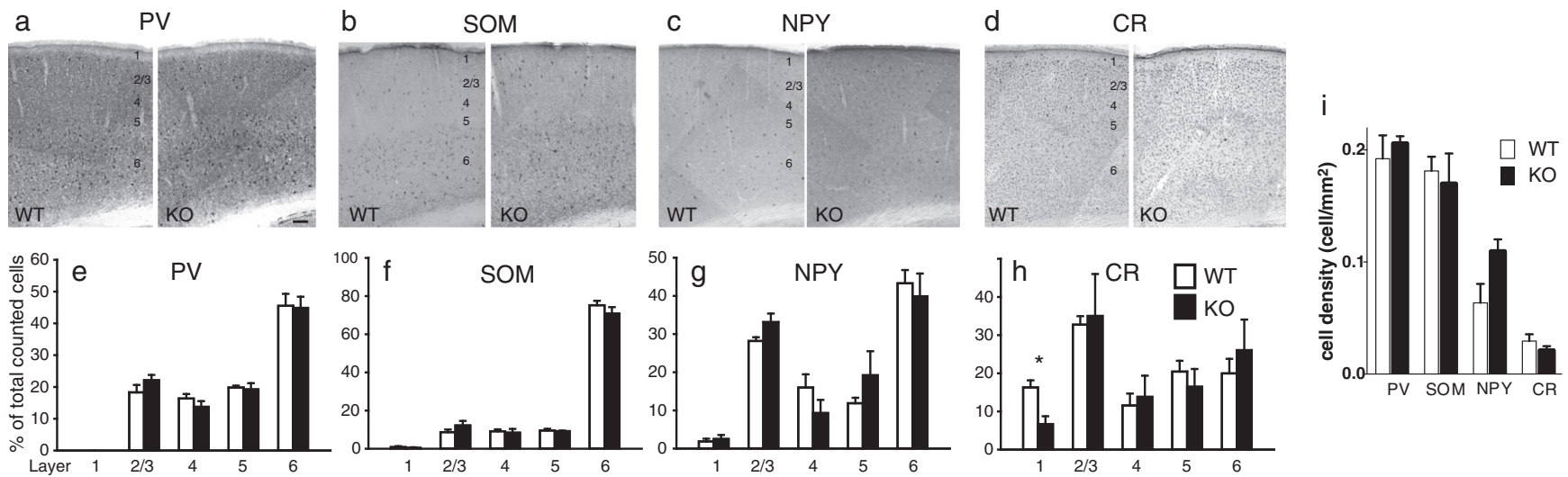
Fig. 3. Laminar position of interneuron subtypes in GABA$_{B1}$R WT and KO mice. a–d. Representative images of PV, SOM, NPY and CR staining show no significant differences in the laminar distribution of interneuron subtypes between WT (left) and KO (right) neocortices. e–h. Summary data showing that the majority of PV + and SOM + cells are localized in L5 and 6. In contrast, a larger percentage of NPY + and CR + cells are found in L1 and 2/3. In KO mice, the percent of total CR + cells is lower in L1. i. Summary histogram shows the cell density of each interneuron subtype assessed within the somatosensory cortex of WT vs. KO mice. (Two way ANOVA, Tukey, $p < 0.05$). PV, SOM and NPY: n = 5 mice were analyzed for each genotype. CR: n = 4 mice were analyzed for each genotype.
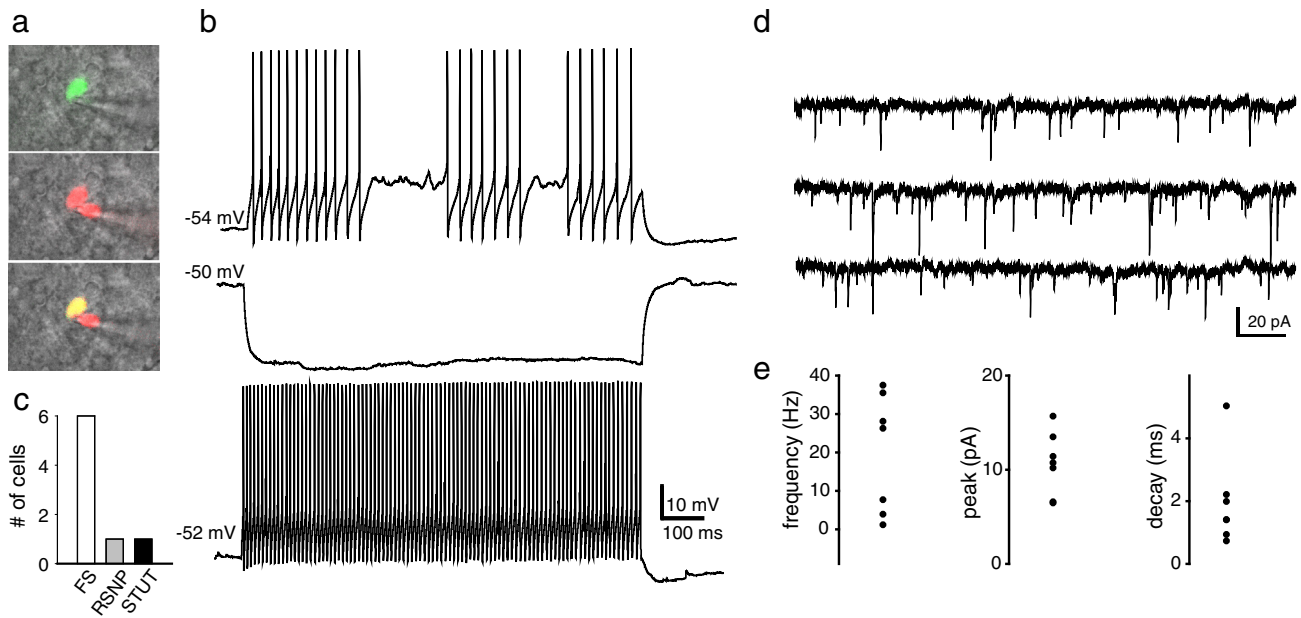
Fig. 4. Grafted KO cells exhibit the electrical footprint of interneurons and receive synaptic input. a. Composite DIC and fluorescent images confirm that the GFP + grafted cell was patched and filled with Alexa 568. The majority of patched cells exhibited a fast spiking cell phenotype (c) as shown in b. All cells subsequently recorded in voltage-clamp exhibited miniature excitatory postsynaptic currents (mEPSCs). The distribution of mEPSC frequency, peak and decay times is shown in e.

layer from which we obtained all recordings, preferentially target inhibitory interneurons (Gonchar and Burkhalter, 1999) potentially consistent with this interpretation. Therefore, it is possible that the reduction in the number of CR + interneurons leads to increased GABA release and extrasynaptic current by disinhibiting interneuron activity. However, we believe that this alternative explanation may be unlikely given that (i) the frequency of inhibitory synaptic currents recorded from KO cells was not elevated relative to WT and (ii) the majority of inhibitory interneurons innervated by CR + terminals are other CR + interneurons (Gonchar and Burkhalter, 1999).

It has been reported that GABA$_{B1}$R KO mice exhibit an epileptic phenotype characterized by electrographic clonic seizures and rare absence and tonic–clonic seizures (Schuler et al., 2001). Using these mice, we observed an elevated tonic current on neocortical pyramidal neurons.
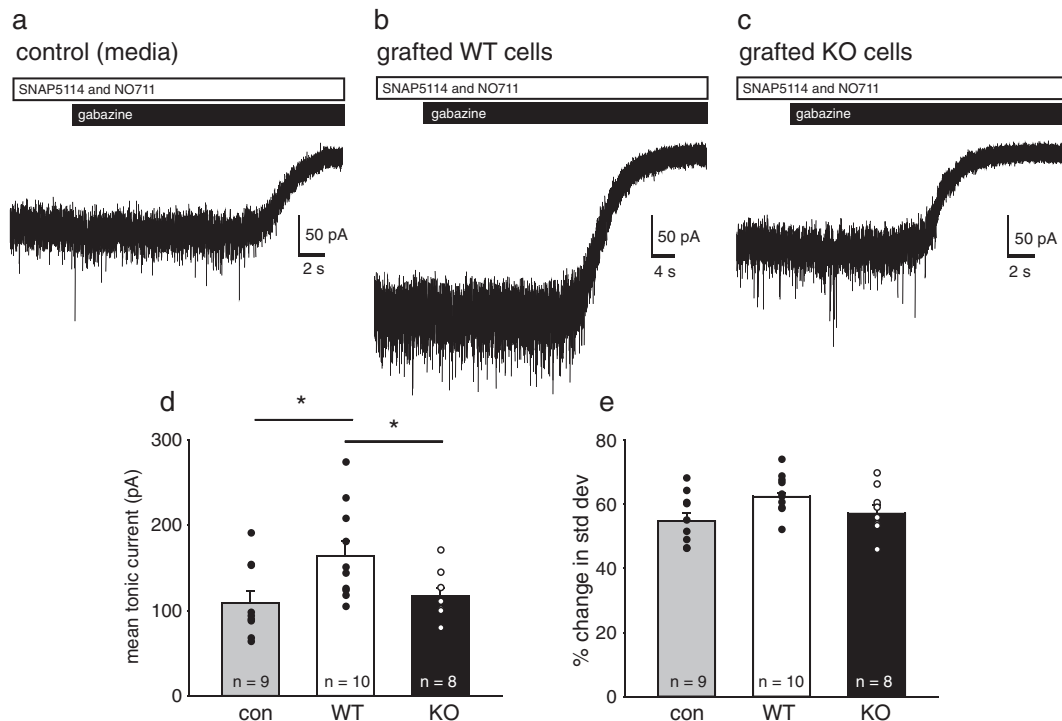
Fig. 5. Host brain tonic inhibition is increased following transplantation of WT, but not KO, MGE cells. a–c. Representative traces of tonic currents recorded from host L2 pyramidal cells. Mice had either received neocortical injections of media (a), WT MGE cells (b) or KO MGE cells (c). Slices were bathed in GABA transporter blockers, SNAP5114 (100 mm) and NO711 (20 mm), followed by the GABA$_A$R antagonist gabazine (100 mm) to reveal the tonic GABA current. d. Summary data showing that mean tonic current is increased following transplantation of WT cells. e. The percent change in standard deviation of the baseline current is not affected by cell transplantation. Two way ANOVA, Tukey, p < 0.05.
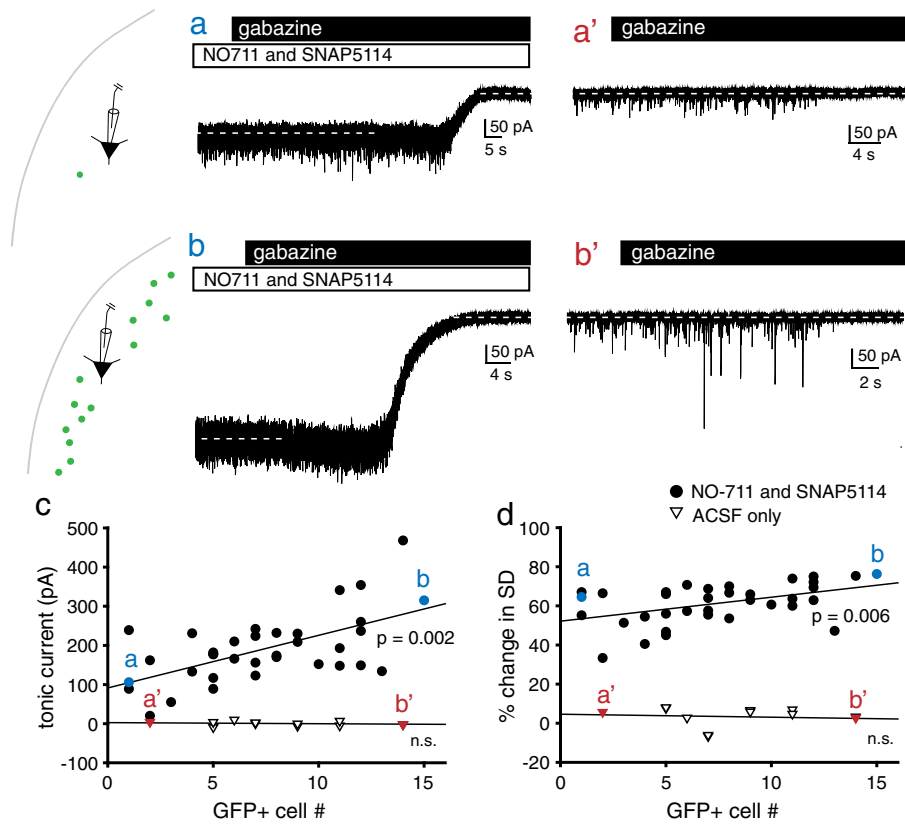
Fig. 6. Tonic current increases with neighboring grafted cell number. a, a′, b, and b′ show representative tonic currents recorded from L2 host pyramidal cells in the presence of NO-711 and SNAP5114 (a and b) or in ACSF only (a′ and b′). Top traces (a and a′) were recorded from cells with only 1 GFP + cell in the same field of view. Bottom traces were recorded from cells with 15 and 14, respectively, GFP + cells in the same field of view. c. Scatter plot of tonic current as a function of the number of grafted cells in the field of view. (•) represents tonic current in the presence of NO-711 and SNAP5114. Spearman Rank correlation coefficient = 0.51, p = 0.002. (▽) represents tonic current in ACSF only (n.s.). d. Scatter plot of the % change in the standard deviation (SD) of the holding current following GABAAR blockade. In the presence of GABA uptake blockers, the change in SD increases with grafted cell number (Spearman Rank correlation coefficient = 0.46, p = 0.006). In both c and d, blue and red data points were obtained from traces shown in a and b vs. a′ and b′, respectively.

That GABA uptake blockers were necessary to reveal tonic currents in both WT and $GABA_{B1}R$ KO mice demonstrates that the GABA uptake mechanisms in the neocortex are quite robust. In contrast, tonic currents are observed in thalamocortical neurons in both WT and established rodent models of absence epilepsy when GABA uptake is intact (Cope et al., 2009). Further, rodent models of epilepsy exhibited elevated tonic current that is likely due to a reduction in GABA uptake caused by GAT1 dysfunction. These studies raise several questions regarding the importance of neocortical tonic currents in the generation of absence seizures. Given that GABA uptake blockers are required to detect tonic currents in neocortical neurons, the relevance of elevated extrasynaptic inhibition in $GABA_{B1}R$ KO mice is unknown. However, we have demonstrated that the powerful GABA uptake mechanisms present in the neocortex play a critical role in minimizing potentially detrimental elevations in tonic current. To compare the relative importance of neocortical vs. thalamocortical neurons in the generation of absence seizures, it is necessary to record tonic currents from neocortical vs. thalamocortical neurons in an established model of absence epilepsy such as the genetic absence epilepsy rats from Strasbourg (Danober et al., 1998).

Effect of interneuron progenitor transplantation on host brain tonic inhibition

Consistent with previous work (Baraban et al., 2009), we demonstrated that transplantation of interneuron progenitors derived from WT MGE donors increased tonic inhibition in the host brain recorded in the presence of GABA uptake blockers. Surprisingly, MGE

transplantation of cells lacking functional $GABA_{B1}Rs$ did not increase host brain tonic inhibition. It is possible that transplanted $GABA_{B1}R$ KO progenitor cells release less GABA and/or disrupt GABA uptake in the host brain following transplantation. It is also possible that presynaptic $GABA_{B1}$ receptors play a critical role in mediating enhanced tonic inhibition seen following MGE cell transplantation possibly by controlling the release of GABA from these cells in a negative feedback manner. Future studies will be necessary to determine the precise mechanism underlying the differential effect of WT and KO progenitors on host brain tonic inhibition.

MGE cell transplantation into the WT cortex increases the frequency of inhibitory synaptic currents recorded from host pyramidal cells (Southwell et al., 2012) and is rapidly emerging as a potential therapeutic intervention for epilepsy (Alvarez-Dolado et al., 2006; Baraban et al., 2009; Howard et al., 2014; Hunt et al., 2013) and schizophrenia (Perez and Lodge, 2013; Tanaka et al., 2011). Given the pro-epileptic consequences of elevated tonic currents, these studies with modification of $GABA_B$ receptor function (Fig. 5) or graft density (Fig. 6) were initiated to determine whether the MGE cell transplantation procedure upwardly scales tonic inhibition within the host brain. Interestingly, we observed a linear increase in tonic inhibition with increased numbers of new GFP^+ interneurons. However, this upward scaling of the tonic current as a function of GFP^+ cell number only occurs when tonic currents are pharmacologically isolated in the presence of GABA transporter blockers. When endogenous GABA uptake mechanisms are functional, neocortical tonic inhibition remains indetectable despite relatively large numbers of new GFP^+ interneurons. Given that elevations in tonic current recorded from thalamocortical neurons induce absence

seizures even in normal rodents (Cope et al., 2009), powerful GABA uptake mechanisms within the neocortex may sub-serve a neuroprotective effect.

Acknowledgments

References

Alvarez-Dolado, M., Calcagnotto, M., Karkar, K., Southwell, D., Jones-Davis, D., Estrada, R., Rubenstein, J., Alvarez-Buylla, A., Baraban, S., 2006. Cortical inhibition modified by embryonic neural precursors grafted into the postnatal brain. J. Neurosci. 26, 7380–7389.

Baraban, S.C., Southwell, D.G., Estrada, R.C., Jones, D.L., Sebe, J.Y., Alfaro-Cervello, C., Garcia-Verdugo, J.M., Rubenstein, J.L., Alvarez-Buylla, A., 2009. Reduction of seizures by transplantation of cortical GABAergic interneuron precursors into Kv1.1 mutant mice. PNAS 106, 15472–15477.

Behar, T., Smith, S., Kennedy, R., McKenzie, J., Maric, I., Barker, J., 2001. GABA(B) receptors mediate motility signals for migrating embryonic cortical cells. Cereb. Cortex 11, 744–753.

Bright, D.P., Smart, T.G., 2013. Methods for recording and measuring tonic GABAA receptor-mediated inhibition. Front. Neural Circ. 7, 193.

Cheah, C., Yu, F., Westenbroek, R., Kalume, F., Oakley, J., Potter, G., Rubenstein, J., Catterall, W., 2012. Specific deletion of NaV1.1 sodium channels in inhibitory interneurons causes seizures and premature death in a mouse model of Dravet syndrome. PNAS 109, 14646–14651.

Ciceri, G., Dehorter, N., Sols, I., Huang, J.Z., Maravall, M., Marin, O., 2013. Lineage-specific laminar organization of cortical GABAergic interneurons. Nat. Neurosci. 16, 1199–1210.

Cobos, I., Calcagnotto, M.E., Vilaythong, A.J., Thwin, M.T., Noebels, J.L., Baraban, S.C., Rubenstein, J.L., 2005. Mice lacking Dlx1 show subtype-specific loss of interneurons, reduced inhibition and epilepsy. Nat. Neurosci. 8, 1059–1068.

Connelly, W., Fyson, S., Errington, A., McCafferty, C., Cope, D., Di Giovanni, G., Crunelli, V., 2013. GABAB receptors regulate extrasynaptic GABAA receptors. J. Neurosci. 33, 3780–3785.

Cope, D.W., Di Giovanni, G., Fyson, S.J., Orban, G., Errington, A.C., Lorincz, M.L., Gould, T.M., Carter, D.A., Crunelli, V., 2009. Enhanced tonic GABAA inhibition in typical absence epilepsy. Nat. Med. 15, 1392–1398.

Danober, L., Deransart, C., Depaulis, A., Vergnes, M., Marescaux, C., 1998. Pathophysiological mechanisms of genetic absence epilepsy in the rat. Prog. Neurobiol. 55, 27–57.

Dutar, P., Nicoll, R., 1988. A physiological role for GABAB receptors in the central nervous system. Nature 332, 156–158.

Fariello, R., Golden, G., 1987. The THIP-induced model of bilateral synchronous spike and wave in rodents. Neuropharmacology 26, 161–165.

Farrant, M., Nusser, Z., 2005. Variations on an inhibitory theme: phasic and tonic activation of GABA(A) receptors. Nat. Rev. Neurosci. 6, 215–229.

Gonchar, Y., Burkhalter, A., 1999. Connectivity of GABAergic calretinin-immunoreactive neurons in rat primary visual cortex. Cereb. Cortex 9, 683–696.

Hosford, D., Clark, S., Cao, Z., Wilson, W., Lin, F., Morrisett, R., Huin, A., 1992. The role of GABAB receptor activation in absence seizures of lethargic (lh/lh) mice. Science 257, 398–401.

Howard, M.A., Rubenstein, J.L., Baraban, S.C., 2014. Bidirectional homeostatic plasticity induced by interneuron cell death and transplantation in vivo. PNAS 111, 492–497.

Hunt, R.F., Girskis, K.M., Rubenstein, J.L., Alvarez-Buylla, A., Baraban, S.C., 2013. GABA progenitors grafted into the adult epileptic brain control seizures and abnormal behavior. Nat. Neurosci. 16, 692–697.

Keros, S., Hablitz, J.J., 2005. Subtype-specific GABA transporter antagonists synergistically modulate phasic and tonic GABAA conductances in rat neocortex. J. Neurophysiol. 94, 2073–2085.

Krook-Magnuson, E., Armstrong, C., Oijala, M., Soltesz, I., 2013. On-demand optogenetic control of spontaneous seizures in temporal lobe epilepsy. Nat. Commun. 4, 1376.

Macdonald, R., Kelly, K., 1995. Antiepileptic drug mechanisms of action. Epilepsia 36 (Suppl. 2), 12.

Marin, O., Rubenstein, J.L., 2001. A long, remarkable journey: tangential migration in the telencephalon. Nat. Rev. Neurosci. 2, 780–790.

Marsh, E., Fulp, C., Gomez, E., Nasrallah, I., Minarcik, J., Sudi, J., Christian, S., Mancini, G., Labosky, P., Dobyns, W., Brooks-Kayal, A., Golden, J., 2009. Targeted loss of Arx results in a developmental epilepsy mouse model and recapitulates the human phenotype in heterozygous females. Brain 132, 1563–1576.

Martinez-Cerdeno, V., Noctor, S.C., Espinosa, A., Ariza, J., Parker, P., Orasji, S., Daadi, M.M., Bankiewicz, K., Alvarez-Buylla, A., Kriegstein, A.R., 2010. Embryonic MGE precursor cells grafted into adult rat striatum integrate and ameliorate motor symptoms in 6-OHDA-lesioned rats. Cell Stem Cell 6, 238–250.

Meldrum, B.S., Rogawski, M.A., 2007. Molecular targets for antiepileptic drug development. Neurotherapeutics 4, 18–61.

Miyoshi, G., Fishell, G., 2011. GABAergic interneuron lineages selectively sort into specific cortical layers during early postnatal development. Cereb. Cortex 21, 845–852.

Miyoshi, G., Butt, S.J., Takebayashi, H., Fishell, G., 2007. Physiologically distinct temporal cohorts of cortical interneurons arise from telencephalic Olig2-expressing precursors. J. Neurosci. 27, 7786–7798.

Miyoshi, G., Hjerling-Leffler, J., Karayannis, T., Sousa, V.H., Butt, S.J., Battiste, J., Johnson, J.E., Machold, R.P., Fishell, G., 2010. Genetic fate mapping reveals that the caudal ganglionic eminence produces a large and diverse population of superficial cortical interneurons. J. Neurosci. 30, 1582–1594.

Nery, S., Fishell, G., Corbin, J.G., 2002. The caudal ganglionic eminence is a source of distinct cortical and subcortical cell populations. Nat. Neurosci. 5, 1279–1287.

Newberry, N., Nicoll, R., 1984. Direct hyperpolarizing action of baclofen on hippocampal pyramidal cells. Nature 308, 450–452.

Perez, S., Lodge, D., 2013. Hippocampal interneuron transplants reverse aberrant dopamine system function and behavior in a rodent model of schizophrenia. Mol. Psychiatry 18, 1193–1198.

Powell, E., Campbell, D., Stanwood, G., Davis, C., Noebels, J., Levitt, P., 2003. Genetic disruption of cortical interneuron development causes region- and GABA cell type-specific deficits, epilepsy, and behavioral dysfunction. J. Neurosci. 23, 622–631.

Scanziani, M., Capogna, M., Gähwiler, B., Thompson, S., 1992. Presynaptic inhibition of miniature excitatory synaptic currents by baclofen and adenosine in the hippocampus. Neuron 9, 919–927.

Schuler, V., Luscher, C., Blanchet, C., Klix, N., Sansig, G., Klebs, K., Schmutz, M., Heid, J., Gentry, C., Urban, L., Fox, A., Spooren, W., Jaton, A.L., Vigouret, J., Pozza, M., Kelly, P. H., Mosbacher, J., Froestl, W., Kaslin, E., Korn, R., Bischoff, S., Kaupmann, K., van der Putten, H., Bettler, B., 2001. Epilepsy, hyperalgesia, impaired memory, and loss of pre- and postsynaptic GABA(B) responses in mice lacking GABA(B(1)). Neuron 31, 47–58.

Sebe, J.Y., Looke-Stewart, E.C., Estrada, R.C., Baraban, S.C., 2010. Robust tonic GABA currents can inhibit cell firing in mouse newborn neocortical pyramidal cells. Eur. J. Neurosci. 32, 1310–1318.

Sebe, J.Y., Looke-Stewart, E.C., Dinday, M., Alvarez-Buylla, A., Baraban, S.C., 2013. Neocortical integration of transplanted GABA progenitor cells from wild type and GABAB receptor knockout mouse donors. Neurosci. Lett. 561, 52–57.

Southwell, D.G., Paredes, M.F., Galvao, R.P., Jones, D.L., Froemke, R.C., Sebe, J.Y., Alfaro-Cervello, C., Tang, Y., Garcia-Verdugo, J.M., Rubenstein, J.L., Baraban, S.C., Alvarez-Buylla, A., 2012. Intrinsically determined cell death of developing cortical interneurons. Nature 491, 109–113.

Tanaka, D., Toriumi, K., Kubo, K.-i., Nabeshima, T., Nakajima, K., 2011. GABAergic precursor transplantation into the prefrontal cortex prevents phencyclidine-induced cognitive deficits. J. Neurosci. 31, 14116–14125.

Thompson, S., Gähwiler, B., 1989. Activity-dependent disinhibition. III. Desensitization and GABAB receptor-mediated presynaptic inhibition in the hippocampus in vitro. J. Neurophysiol. 61, 524–533.

Wang, Y., Dye, C.A., Sohal, V., Long, J.E., Estrada, R.C., Roztocil, T., Lufkin, T., Deisseroth, K., Baraban, S.C., Rubenstein, J.L., 2010. Dlx5 and Dlx6 regulate the development of parvalbumin-expressing cortical interneurons. J. Neurosci. 30, 5334–5345.

Wichterle, H., Garcia-Verdugo, J.M., Herrera, D.G., Alvarez-Buylla, A., 1999. Young neurons from medial ganglionic eminence disperse in adult and embryonic brain. Nat. Neurosci. 2, 461–466.